Applied Catalysis B: Environmental 144 (2014) 189–195

Contents lists available at ScienceDirect

Applied Catalysis B: Environmental

journal homepage: www.elsevier.com/locate/apcatb

TiO_2-photocatalytic transformation of Cr(VI) in the presence of EDTA: Comparison of different commercial photocatalysts and studies by Time Resolved Microwave Conductivity

Jorge M. Meichtry[a,b], Christophe Colbeau-Justin[c,d], Graciela Custo[a], Marta I. Litter[a,b,e,*]

[a] Gerencia Química, Comisión Nacional de Energía Atómica, Av. Gral. Paz 1499, 1650 San Martín, Prov. de Buenos Aires, Argentina
[b] Consejo Nacional de Investigaciones Científicas y Técnicas, Av. Rivadavia 1917, 1033 Ciudad Autónoma de Buenos Aires, Argentina
[c] Univ. Paris-Sud, Laboratoire de Chimie Physique, UMR8000, Orsay 91405, France
[d] CNRS, Laboratoire de Chimie Physique, UMR8000, Orsay 91405, France
[e] Instituto de Investigación e Ingeniería Ambiental, Universidad de Gral. San Martín, Peatonal Belgrano 3563, 1er. piso, 1650 San Martín, Prov. de Buenos Aires, Argentina

ARTICLE INFO

Article history:
Received 20 February 2013
Received in revised form 31 May 2013
Accepted 28 June 2013
Available online 7 July 2013

Keywords:
Cr(VI)
Cr(III)
EDTA
TiO_2-heterogeneous photocatalysis
Time Resolved Microwave Conductivity (TRMC)

ABSTRACT

The photocatalytic efficiency for Cr(VI) transformation in the presence of etilendiaminetetraacetic acid (EDTA) at pH 2 over various commercial TiO_2 samples (Evonik P25, Cristal Global PC50, PC100 and PC500, Hombikat UV100, Fluka and Kemira S230) was evaluated. The decay was adjusted to a pseudo-first order kinetics in all cases and the photocatalytic activity of the samples was estimated from the kinetic constants. The order of the photocatalytic activity was PC500 ≅ UV100 > P25 ≅ PC100 > S230 ≅ PC50 ≫ Fluka and it strongly depends on the nature of the TiO_2 samples, especially on the specific surface area, except for S230 and for P25. The formation of the Cr(III)–EDTA complex in solution as a product of the Cr(VI) photocatalytic reduction was confirmed by visible spectrophotometry. Simultaneous kinetics of Cr(VI) reduction and of Cr(III)–EDTA formation has been determined for the first time and the results indicate that evolution of both species are related. TRMC measurements were applied for the first time to a reductive heterogeneous photocatalytic reaction of a metal ion system, and the experimental results were adjusted to a power law decay, relating the data to those of the photocatalytic experiments.

1. Introduction

The photocatalytic reduction of Cr(VI) in water has been widely reported in the literature [1–3], both as an environmentally friendly process for the treatment of this pollutant [4–16] [1] as well as a simple system to evaluate the photocatalytic activity of various semiconductors [11,12,14,17–29]. This photocatalytic system, where Cr(III) is the final stable product, is unique: Cr(VI) is the only metal species whose reductive TiO_2-photocatalytic removal is not influenced by the presence of oxygen, at least at acid pH, in contrast with most metals, explained by the fast capture of electrons caused by a very strong association between Cr(VI) and TiO_2 through a charge-transfer complex [9,30]. However, the influence of the physical properties of the photocatalyst samples used in the reaction is still under discussion and, from the point of view of photocatalysts offered in the market, this aspect should be analyzed.

Time Resolved Microwave Conductivity (TRMC) is a powerful tool for analyzing charge carrier lifetimes in TiO_2 [31–34]. The technique can be used also to understand the effect of species adsorbed or deposited on the surface of a semiconductor [35–38].

In this paper, the photocatalytic activity of various commercial TiO_2 samples, i.e., Evonik P25, Cristal Global PC50, PC100 and PC500, Hombikat UV100, Fluka and Kemira S230 was evaluated, and the results were related to those of TRMC measurements for the most representative samples.

2. Experimental

2.1. Chemicals and materials

P25 (Evonik), Hombikat UV100 (Sachtleben Chemie), PC50, PC100 and PC500 (Cristal Global), reagent TiO_2 (Fluka, 99%) and Finn-Ti S230 (Kemira) were used as received.

* Corresponding author at: Gerencia Química, Comisión Nacional de Energía Atómica, Av. Gral. Paz 1499, 1650 San Martín, Prov. de Buenos Aires, Argentina. Tel.: +54 11 67727016; fax: +54 11 677278816.
E-mail addresses: litter@cnea.gov.ar, marta.litter@gmail.com (M.I. Litter).

[1] Only references from the last ten years are given.

0926-3373/$ – see front matter © 2013 Elsevier B.V. All rights reserved.
http://dx.doi.org/10.1016/j.apcatb.2013.06.032

Potassium dichromate was Prolabo (99.9%), and disodium etilendiaminetetraacetic acid (Na_2EDTA, 99%) was Merck. Nitric acid (68%, Prolabo) was used for pH adjustment. All other reagents were of analytical grade and used as received. All solutions and suspensions were prepared with distilled water.

Filtration of suspensions was performed through 0.2 μm Interchim cellulose acetate filters, 25 mm diameter.

2.2. Preparation of suspensions and TRMC samples

To prepare the suspensions to be irradiated, the following procedure was used: 200 mL of water were added to 0.25 g of TiO_2 in a 250 mL volumetric flask; then, the corresponding amount of a 10 mM Cr(VI) solution was added to get a final 0.8 mM concentration, and pH was adjusted to 2 with 1 M HNO_3; in the corresponding experiments, solid Na_2EDTA to get a 2 mM final concentration was introduced before adjusting the pH. Water was added in all cases to complete 250 mL. The suspension was ultrasonicated for 2 min, and 200 mL were used in each photocatalytic experiment, keeping the remaining 50 mL in the dark for 30 min to ensure adsorption equilibrium before irradiation; after filtration, the amount of Cr(VI) adsorbed onto the photocatalyst in this 50 mL suspension was measured and discounted from the initial concentration to evaluate changes in concentration due only to irradiation.

For TRMC measurements, the pure samples were evaluated directly as powders. To measure Cr(VI)-modified TiO_2 photocatalysts, samples were suspended at 1 g L^{-1} in 0.8 mM Cr(VI) solutions at pH 2 (HNO_3) (with EDTA in the indicated cases), stirred in the dark for 60 min and centrifuged for 10 min at 10,000 rpm. The supernatant was eliminated, the samples were dried at 35 °C for 24 h, and then stored in the dark. Blanks with water at pH 2 adjusted with 1 M (HNO_3-modified TiO_2) were also prepared.

2.3. Photocatalytic runs

Irradiation runs were performed in a Pyrex recirculating batch annular photoreactor, 160 mm length, 40 mm outer diameter and 30 mm inner diameter. Inside the inner tube, an 8 W Philips fluorescent black light lamp was placed, fed by a 15 W ballast. This lamp emits predominantly at 365 nm. A TiO_2 suspension (200 mL) was poured in a glass reservoir and continuously recirculated (600 mL min^{-1}) to the photoreactor by means of a peristaltic pump. The irradiated volume in the photoreactor was 110 mL. The system was freely open to the air because, as reported, molecular oxygen does not interfere with the Cr(VI) photocatalytic reduction over TiO_2 under acidic conditions [1,2]. The whole setup was thermostatted at 298 K. The total incident photon flux, $q^0_{n,p}/V$, determined by potassium ferrioxalate actinometry, was 95 μeinstein s^{-1} L^{-1}, using the same conditions of flow rate and volume as in the experiments.

The experiments were performed at least by duplicate and the standard deviation among replicates was never higher than 10%.

2.4. Analytical determinations

For the spectrophotometric determinations, samples (1 mL) were taken from the reservoir, filtered and brought to 10 mL with water. Cr(VI) was determined by measuring the absorbance at 352 nm [39]. The more sensible but more complicated diphenylcarbazide method was found not necessary for these Cr(VI) concentrations [8]. The concentration of Cr(III)-EDTA in solution was measured at 540 nm as previously reported, using $\varepsilon = 14\ m^2\ mol^{-1}$ [40]. Neither free Cr(III) [40,41] nor Cr(VI) species [4,30,42] interferes at this wavelength. However, Cr(III) can form complexes with ethylenediamine-N,N′-triacetic acid (ED3A) [42], ethylenediaminediacetic acid (EDDA) [43] ethylenediaminemonoacetic acid (EDMA) [44] and iminodiacetic acid (IDA) [45], having UV–vis spectra similar to that of Cr(III)-EDTA, with maximum ε values also at 540 nm and in the same order of magnitude (6–13 $m^2\ mol^{-1}$). These compounds have been found as products of EDTA photocatalytic degradation, although reported to be formed in very low amounts [46,47]. Therefore, it will be assumed that the measured absorbance corresponds only to the Cr(III)-EDTA complex, affected by some minor error without influence on our conclusions. A double-beam Varian UV–vis recording spectrophotometer, model Cary UV 300, was used for the spectrophotometric measurements, and calibration curves were obtained in all cases.

Total Cr content on TiO_2 either before or after irradiation was determined by Wavelength Dispersive X-Ray Fluorescence (WDXRF) measurements, using a Venus 200 MiniLab, Panalytical WDXRF equipment with a Sc anode X-Ray tube. The excitation conditions were 50 kV and 4 mA. As thermal Cr(VI) reduction by EDTA can take place during the drying process of the samples [40], the amount of Cr on TiO_2 before irradiation was determined before the addition of the organic compound. The amount of Cr in the TiO_2 samples was expressed as equivalent concentration (mmol of Cr/g of TiO_2), i.e., as the concentration of total Cr (mM) in a suspension containing 1 g L^{-1} of TiO_2. The samples were initially prepared as described for the TRMC measurements, mixing them at the end with cellulose (40% TiO_2–60% cellulose) and compressing the mixture in order to obtain a pellet. The calibration curves were prepared similarly by mixing pure P25 with the corresponding amount of Cr(VI) in water.

2.5. BET area measurements

Measurements were carried out by N_2 adsorption at 77 K (molecular surface area 0.162 nm^2) on a Micromeritics ASAP 2020 equipment. Before analysis, the samples were heated under vacuum at 373 K for 8 h.

2.6. TRMC measurements

Measurements were carried out in the Helmholtz Zentrum Berlin (Germany) with the experimental setup described previously [31]. The incident microwaves were generated by a Gunn diode of the K_a band (28–38 GHz) and the experiments were performed at 31.4 GHz. Pulsed light source was a Nd:YAG laser providing an IR radiation at $\lambda = 1064$ nm. Full-width at half-maximum (FWHM) of one pulse was 10 ns; repetition frequency of the pulses was 10 Hz. UV light (355 nm) was obtained by tripling the IR radiation. The light energy density received by the sample was 1.3 mJ cm^{-2}. In order to have a more accurate value of the signal at the maximum (I_{max}) and at 40 ns after the maximum (I_{40ns}), the values reported for both parameters were averaged within ±5 ns of the corresponding time. The uncertainty of the measurements was of 0.005 V for times shorter than 100 ns (i.e. when the signal is maximum), and of 0.001 V for longer times.

3. Results and discussion

3.1. Photocatalytic experiments of Cr(VI) decay with different TiO_2 samples

In Table 1, some physical properties of the TiO_2 samples used in this work are indicated, with BET area values measured in our laboratories and compared with reported values taken from the literature [4,12,17,37,48–52].

In Fig. 1, results of the photocatalytic decay of Cr(VI) (0.8 mM) in the presence of EDTA (2 mM) at pH 2 using different TiO_2 samples (1 g L^{-1}) are shown. These conditions were chosen according to results obtained in previous works to warrant a low Cr(VI) filter

Table 1
Some physical properties of the TiO_2 samples.

Sample	Particle size (nm)	SSA measured ($m^2\ g^{-1}$)	SSA from literature ($m^2\ g^{-1}$)	Phases
P25	20–50	54.7 ± 0.3	48–56	A (70–80%) R (30–20%)
PC50	20–40	45.7 ± 0.2	50	A
PC100	18–21	82.4 ± 0.3	89	A
PC500	5–10	306 ± 2	287–350	A
UV100	5–13	300 ± 2	250–300	A
Fluka	100–400	8.30 ± 0.01	9	A
S230	4–7	270.5 ± 0.5	230	A

A: anatase; R: rutile.

effect and a pseudo-first order decay [8,29]. All experiments were continued until total Cr(VI) transformation; as can be seen, reactivity is extremely high, with total conversion of Cr(VI) in less than 300 s over almost all photocatalyst samples; the Fluka sample was the less active, requiring $t = 1800$ s for the complete Cr(VI) decay (see inset of Fig. 1). So far, no photocatalytic data with S230 have been reported, while there is only one report regarding Fluka [50], where the efficiency of this material was found much lower than that of P25, PC50 and PC500, in agreement with the results here obtained. The temporal evolution of the normalized Cr(VI) concentration ($[Cr(VI)]/[Cr(VI)]_0$) could be fitted to Eq. (1):

$$\frac{[Cr(VI)]}{[Cr(VI)]_0} = \exp^{-k_c \times t} \quad (1)$$

where k_c is the pseudo-first order kinetic constant.

The spectra of samples during the runs confirmed the formation of Cr(III)-EDTA as the final product by the appearance of two peaks at 390 and 540 nm [42,53]. The experimental data of the Cr(III)–EDTA temporal evolution (Fig. 2, with inset for Fluka at longer times) were fitted to Eq. (2):

$$[Cr(III) - EDTA] = C_\infty \times (1 - \exp^{-k_f \times t}) \quad (2)$$

where C_∞ is the amount of Cr(VI) transformed into Cr(III)–EDTA at the end of the reaction, and k_f is the pseudo-first order kinetic constant for the complex formation.

In Table 2 are shown the kinetic parameters of all curves extracted from Figs. 1 and 2, together with the amount of Cr onto the photocatalyst before (i.e., adsorbed, in the absence of EDTA) and after irradiation (in the presence of EDTA), expressed in equivalent Cr concentration.

As previously postulated, the photocatalytic reduction of Cr(VI) under regular illumination takes place through three successive one-electron reduction steps[2], ending in Cr(III) [1,2]. After the mentioned strong association through the Cr(VI)–TiO_2 complex [9,30], the first step is the attack of CB or trapped electrons to Cr(VI) to yield Cr(V), a thermodynamically highly feasible process on the TiO_2 surface in water suspension, considering the reduction potential of the couple in homogeneous water solution ($E^0 = +0.55$ V [54] [3]), and the redox levels of electrons and holes ($E^0 = -0.3$ and +2.9 V, respectively for P25 [55]). A similar process can be proposed on the wet and dried TiO_2 surface [30]:

$$Cr(VI)\text{–}TiO_2 + e_{CB}^-/e_{tr}^- \rightarrow Cr(V) \quad (3)$$

The conjugate reaction is water or EDTA oxidation depending on the conditions:

$$H_2O + h_{VB}^+/h_{tr}^+ \rightarrow HO^\bullet + H^+ \quad (4)$$

$$RCH_2COOH + h_{VB}^+/h_{tr}^+ \rightarrow RCH_2COO^\bullet + H^+ \rightarrow\rightarrow CO_2 + RCH_2^\bullet + e^- \quad (5)$$

$$RCH_2COOH + h_{VB}^+/h_{tr}^+ \rightarrow RCH^\bullet COOH + H^+ \rightarrow\rightarrow CO_2 + RCH_2^\bullet + e^- \quad (6)$$

In the absence of EDTA, P25 was found to be more active than UV100 for Cr(VI) removal [13,17], but the opposite occurred in the presence of EDTA, as confirmed here (Fig. 1 and Table 2).

According to Table 2, the order of reactivity toward Cr(VI) reduction is PC500 ≅ UV100 > P25 ≅ PC100 > S230 ≅ PC50 ≫ Fluka. Therefore, with the exception of S230, the efficiency in the presence of EDTA increases with the increase of the specific surface area (SSA, Table 1, Fig. S1(a), supporting information section), in agreement with previous papers of the system in the presence of electron donors [4,6,22,24,64], although there is no large influence for the highest areas. As expected, the same trend is observed regarding the amount of Cr on TiO_2 (Table 1, Fig. S1(b), supporting information section). In contrast, in the absence of donors, the SSA does not seem to be the key parameter [4,6,17,24,56,64].

Except for P25, k_c and k_f have almost the same value, indicating that Cr(VI) and Cr(III)–EDTA evolution are closely related, the lifetime of Cr intermediate species being negligible. The difference between k_c and k_f in the case of P25, especially since the amounts of total Cr(III)–EDTA and Cr on TiO_2 after irradiation are similar to those obtained for the other catalysts (excepting Fluka), can be explained by a different initial reactivity on rutile and anatase active sites.

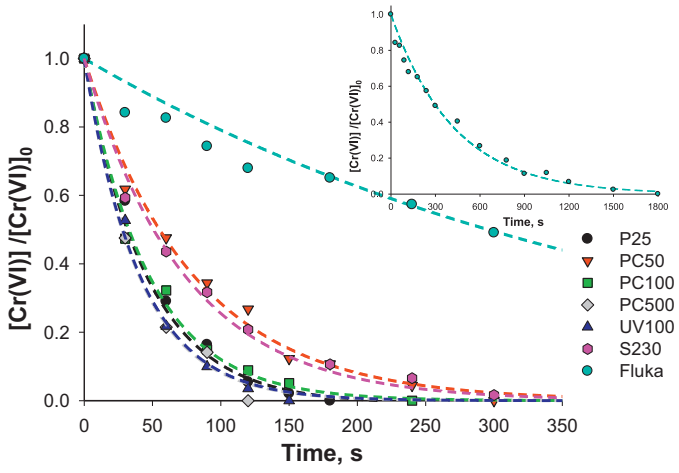

Fig. 1. Photocatalytic decay of Cr(VI) over different TiO_2 samples. Experimental conditions: $[Cr(VI)]_0 = 0.8$ mM, $[EDTA]_0 = 2$ mM, pH 2 (HNO_3), $[TiO_2] = 1$ g L^{-1}, $V_{suspension} = 200$ mL, $q^0_{n,p}/V = 95$ μeinstein s^{-1} L^{-1}. Dashed lines are the fitting of the experimental points with Eq. (1). Inset: data for Fluka up to 1800 s.

[2] However, it should be taken into account that if the TiO_2 sample is irradiated with a laser, accumulation of electrons and changes in the Fermi level of the semiconductor can take place, leading to multielectronic processes.

[3] All standard reduction potentials vs. NHE.

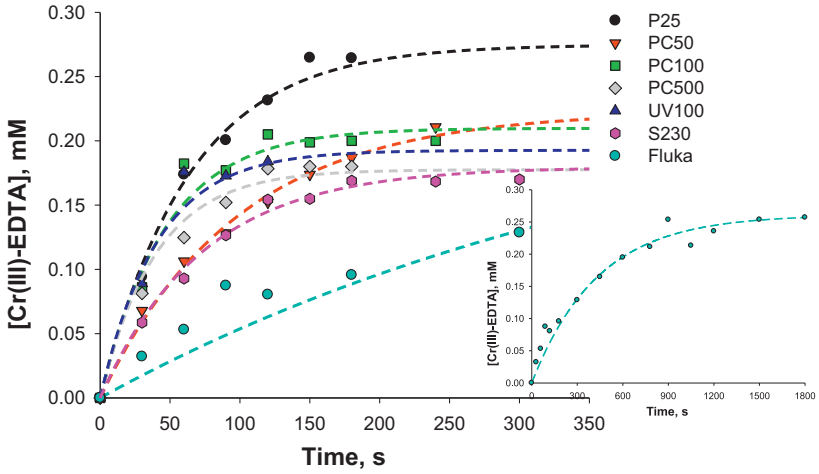

Fig. 2. Temporal evolution of Cr(III)–EDTA under conditions of Fig. 1. Dashed lines are the fitting of the experimental points with Eq. (2). Inset: data for Fluka up to 1800 s.

Figs. 1 and 2 indicate that, although Cr(VI) is completely transformed in all samples at 300 s (with the exception of Fluka), only the C_∞ fraction of the initial reduced Cr(VI) is transformed into Cr(III)–EDTA at the end of the reaction; the difference can be assigned to the formation of other Cr(III) aqueous species with lower absorbance at 540 nm, and to Cr(III) retained on the TiO_2 surface, as observed by the green color onto the solid surface. This effect was also noticed in previous works [3,8,56,57].

Table 2 and Fig. S2 show that the amount of adsorbed Cr(VI) increases almost linearly with SSA. In contrast, the equivalent Cr concentration after irradiation (14–21% of the initial Cr(VI) concentration) does not show a clear relationship with SSA (dashed line in Fig. S2). This can be related to the rather constant C_∞ values (Table 2), indicating that the speciation of Cr(III) products is almost independent of the catalyst used. The only exception was Fluka, where less than 5% of the initial Cr(VI) was retained on the surface, in accordance with its higher C_∞ value.

3.2. TRMC results

Fundamentals for TRMC have been reported elsewhere [31–33,37,38]. Briefly, this technique is based on the measurement of the change of the microwave power reflected by a solid sample, $\Delta P(t)$, induced by its laser-pulsed illumination. The relative difference $\Delta P(t)/P$ can be correlated to the difference of conductivity $\Delta\sigma(t)$ according to [31]:

$$\frac{\Delta P(t)}{P} = A\Delta\sigma(t) = Ae\sum_i \Delta n_i(t)\mu_i \quad (7)$$

where A is a sensitivity factor, e is the electron charge, $\Delta n_i(t)$ is the number of excess charge carriers i at time t, and μ_i is their mobility. In the specific case of TiO_2, Δn_i is reduced to electrons in the conduction band because their mobility is much larger than that of the holes [31,32].

The main data provided by TRMC are the maximum value of the signal (I_{max}), which indicates the number of the excess charge carriers created by the UV pulse, including decay processes during the excitation by the laser (10 ns), and the decay ($I(t)$) due to the decrease of the excess electrons, either by recombination or trapping processes. Concerning the decay, i.e. the lifetime of charge carriers, a short and a long range are usually analyzed. The short-range decay, arbitrarily fixed up to 40 ns after the beginning of the pulse, represented by the I_{40ns}/I_{max} ratio, reflects fast processes, mainly recombination of charge carriers, a high value indicating a low recombination speed [36]. The long-range decay, here fixed after 200 ns, is related to slow processes involving trapped species, i.e., interfacial charge transfer reactions and decay of excess electrons controlled by the relaxation time of trapped holes [57]. In this range, the decay of the TRMC signal can be fitted to a power decay according to:

$$I = I_D \times t^{-k_D} \quad (8)$$

where I_D is the intensity of the signal due to charge carriers that recombine after 200 ns, and k_D is an adimensional parameter related to their lifetime: higher k_D values correspond to faster decays of the TRMC signal [31,36]. Similar I_{max} and I_D values indicate that charge carriers decay only by slow processes.

The relationship between TRMC parameters and photocatalytic activity for pure TiO_2 samples has been verified in previous works [31,32,36,37]. High I_{max} indicate a large amount of created

Table 2
Kinetic parameters for the Cr(VI) decay extracted from Fig. 1 calculated with Eq. (1), for Cr(III)–EDTA formation extracted from Fig. 2 calculated with Eq. (2), and equivalent Cr concentration per 1 g L^{-1} of TiO_2.

Sample	$k_c \times 10^3$ (s^{-1})	R^2	$k_f \times 10^3$ (s^{-1})	C_∞ (mM)	R^2	Cr on TiO_2 (mmol g^{-1}) b.i.[a,b]	Cr on TiO_2 (mmol g^{-1}) a.i.[c]
P25	21.7 ± 0.7	0.993	16.0 ± 1.4	0.22 ± 0.01	0.992	0.05	0.11
PC50	12.6 ± 0.6	0.986	10.2 ± 0.7	0.22 ± 0.01	0.995	0.03	0.13
PC100	21.2 ± 1.1	0.992	21.3 ± 3.7	0.21 ± 0.01	0.964	0.05	0.12
PC500	25.1 ± 1.4	0.994	25.1 ± 1.4	0.18 ± 0.01	0.982	0.35	0.17
UV100	24.6 ± 1.1	0.994	24.4 ± 1.1	0.19 ± 0.01	0.968	0.30	0.11
Fluka	2.3 ± 0.10	0.992	2.3 ± 0.30	0.26 ± 0.01	0.966	0	0.03
S230	13.7 ± 0.7	0.992	13.7 ± 0.2	0.18 ± 0.01	0.992	0.19	0.15

[a] Determined before EDTA addition.
[b] b.i.: before irradiation.
[c] a.i.: after irradiation.

charge-carriers, while long lifetimes reveal good charge-carrier transport properties, good crystallinity and lack of defects in the photocatalyst [32,34]; a small crystalline size and a high area have been related with high k_D values [32,34].

Adsorbed or deposited species on the photocatalyst surface influence the TRMC signal, according to three different effects [37]. First, by absorbing photons that hinder the creation of charge carriers by acting as a shield or UV filter for TiO_2; this decreases I_{max} and I_D but do not affect lifetimes. A second effect is their behavior as impurities or defects, giving rise to faster recombination processes; this decreases all TRMC parameters. A third effect is the occurrence of interfacial charge transfer processes between the charge carriers and the adsorbed species; this changes especially TRMC parameters related to long times [36]. The three phenomena occur simultaneously, the first two being detrimental for the activity, while the third one being favorable.

Other phenomena more related to the specific structural nature of the materials affect photoactivity, SSA being one of the most relevant as a high SSA induces a high number of accessible active sites. Especially, when a strong adsorbate is present on the TiO_2 surface, SSA can become the key factor to explain the photocatalytic activity [5,51] and the TRMC results. Surface treatments lead, generally, to a decrease of I_{max} [36].

In this work, TRMC measurements were performed with samples in the following conditions: i) pure, unmodified TiO_2 samples, ii) samples previously suspended at $1\,g\,L^{-1}$ in HNO_3 at pH 2, iii) samples previously suspended in 0.8 mM Cr(VI) at pH 2 (HNO_3), and iv) samples filtered after irradiation in the presence of EDTA (conditions of Fig. 1) when all the initial Cr(VI) has been reduced to Cr(III). TiO_2 samples suspended in HNO_3 served as a blank to indicate the influence of nitrate on TRMC results. As an example, results for P25 are shown in Fig. 3, where the temporal variation of the TRMC signal I is plotted. Results for UV100 and for PC samples are similar, and are displayed in Figs. S3–S6. This analysis has been not performed for Fluka and S230, and for PC100 and PC500 after irradiation in the presence of Cr(VI)/EDTA.

TRMC data are presented in Table 3. I_{max} and I_{40ns}/I_{max} are directly extracted from Figs. 3 and S3 to S6. Concerning I_D and k_D, a good fitting to Eq. (8) was obtained ($R^2 > 0.99$) when $I \geq 0.01$ V; with lower I values, the signal became noisy and the R^2 values decreased, although the tendency remained.

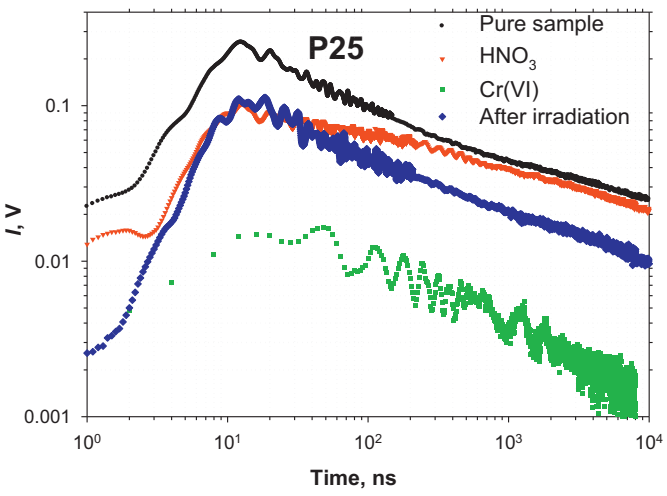

Fig. 3. TRMC measurements of P25 in different conditions. Pure sample: unmodified TiO_2. HNO_3: P25 previously suspended at $1\,g\,L^{-1}$ in HNO_3 at pH 2. Cr(VI): TiO_2 previously suspended at $1\,g\,L^{-1}$ in 0.8 mM Cr(VI) at pH 2 (HNO_3). After irradiation: P25 after irradiation in conditions of Fig. 1.

3.3. Pure samples

Previous studies [31,33,34,37], comparing commercial TiO_2 samples (P25, PC50 and UV100), reported that an increase of SSA and a decrease of particle size cause a decrease on I_{max} and I_{40ns}/I_{max}, due to the lower crystallinity and higher fast electron–hole recombination. This feature is clearly seen here. PC50 and PC100 present the highest TRMC values, while PC500 and UV100 present the lowest ones, P25 being intermediate. As observed before [37], although PC50 and P25 have similar BET area and particle size, decay in P25 is faster due to the presence of the rutile phase [32].

Table 1 shows that particle size and SSA of PC100 and PC50 are similar; this can account for their almost identical I_{max} and

Table 3
TRMC parameters for pure and modified TiO_2 samples extracted from Figs. 5 and S1 to S4.

Sample/condition	I_{max} (V)	$I_{40\ ns}/I_{max}$ (V)	I_D (V)	k_D
pure P25	0.226	0.538	0.133	0.259
P25/HNO_3	0.096	0.774	0.105	0.252
P25/Cr(VI)	0.015	0.676	0.017	0.478
P25/Cr(VI) after irradiation	0.102	0.558	0.077	0.307
pure PC50	0.282	0.640	0.216	0.226
PC50/HNO_3	0.235	0.598	0.168	0.241
PC50/Cr(VI)	0.266	0.587	0.204	0.259
PC50/Cr(VI)/after irradiation	0.179	0.567	0.139	0.268
pure PC100	0.283	0.638	0.290	0.382
PC100/HNO_3	0.227	0.603	0.187	0.331
PC100/Cr(VI)	0.171	0.325	0.058	0.273
PC100/Cr(VI)after irradiation	ND	ND	ND	ND
pure PC500[a]	0.110	0.223	0.090	0.816
PC500/HNO_3[a]	0.096	0.215	0.092	0.930
PC500/Cr(VI)[a]	0.010	>0.1	–[b]	–[b]
PC500/Cr(VI) after irradiation[a]	ND	ND	ND	ND
pure UV100	0.102	0.288	0.036	0.576
UV100/HNO_3	0.066	0.262	0.030	0.572
UV100/Cr(VI)[b]	–	–	–	–
UV100/Cr(VI) after irradiation	0.063	0.319	0.019	0.300

ND: not determined.
[a] Analysis for PC500 was performed in all cases until 10^3 ns.
[b] No analysis of the TRMC signal could be performed due to the negligible intensity of the signal.

I_{40ns}/I_{max}; however, the similar I_{max} and I_D of PC100 suggest that charge carriers decay in this sample mainly by slow processes, and this can be assigned to the smaller crystalline size and higher area of this sample compared with PC50. On the other hand, the smaller crystalline size and higher area of PC500 and UV100 (Table 1) account for the smaller I_{max}, I_{40ns}/I_{max} and higher k_D.

3.4. Treated samples

Table 3 shows that both the treatment with HNO_3 and with Cr(VI) in HNO_3 decrease I_{max} and I_{40ns}/I_{max} in all TiO_2 samples.

At the working pH, nitrate is chemisorbed onto the TiO_2 surface generating species like $>Ti^{IV}–ONO_2$ [55]. As nitrate does not absorb the laser emission (355 nm), a filter effect is not expected. The decrease of I_{max} and I_D can be explained by chemisorbed HNO_3 behaving as an impurity. An interfacial charge transfer process after irradiation by the laser pulse can be also envisaged, with nitrate oxidation by holes:

$$NO_3^- + h_{VB}^+/h_{tr}^+ \rightarrow NO_3^\bullet \quad (9)$$

or by reduction by electrons:

$$NO_3^- + e_{CB}^-/e_{tr}^- \rightarrow NO_3^{2-} \quad (10)$$

Reaction (9) is thermodynamically feasible ($E^0 = 2.3$ V [58]), but reaction (10) is not possible ($E^0 = -0.89$ V [59], see however footnote 2 in page 3 as nitrate can be transformed through multielectronic processes [60]), especially because this reaction requires an anoxic atmosphere, which was not the case. The decrease of the TRMC signal by adsorbed HNO_3 was previously reported [55], associated to a more efficient and faster e_{CB}^-/h_{VB}^+ recombination. Thus, the lowering of I_{max} by nitrate is due to hole trapping according to Eq. (9), followed by a channel for recombination through [55]:

$$NO_3^\bullet + e_{CB}^-/e_{tr}^- \rightarrow NO_3^- \quad (11)$$

In any case, the main influence of HNO_3 is on I_{max} and I_D and less on I_{40ns}/I_{max} and k_D. The trend in TRMC parameters is similar to that of the pure samples (Section 3.2.1). P25 remains peculiar, with a rather much higher I_{40ns}/I_{max} than the pure sample, although this effect could be more related to the decrease on I_{max} than to an increase in I_{40ns}.

The effect of Cr(VI) is more notable than that of HNO_3. As the amount of adsorbed nitrate is expected to be lower in the presence of Cr(VI) due to competition for the TiO_2 active sites, a lower contribution of NO_3^- to the TRMC signal is expected. The decrease of I_{max} in almost all Cr(VI)-modified samples (no irradiation) is more significant in the samples with higher SSA, i.e. having more adsorbed Cr(VI) (Table 2), with the smallest effect observed for PC50 and the highest one for PC500 and UV100. As stated before, this effect can be related to: i) a decrease of the light reaching the TiO_2 particles, due to the filter effect of the Cr(VI)–TiO_2 complex [9,30]; ii) to recombination provoked by Cr(VI) behaving as an impurity or iii) the transfer of electrons to adsorbed Cr(VI) (reaction (3)) [31,37,55]. It can be proposed that the fast electron transfer to Cr(VI) is the main effect decreasing I_{max}.

The increase of the Cr(VI) surface concentration before irradiation (Table 2, Fig. S2) has also a strong influence on I_D and, to a lower extent, on k_D, with a more pronounced effect again for PC500 and UV100, where a very small or no signal at all is observed. The main effect at long times is probably the rapid capture of e_{CB}^- by Cr(VI), higher with higher SSA. A similar behavior was found in the photocatalytic reduction of Se(IV) and Se(VI) in the presence of formic acid, where PC500 showed a higher photocatalytic activity than P25 and PC50 [61]; this system is comparable to Cr(VI)/EDTA, where both donor and acceptor are adsorbed on TiO_2. It can be concluded that in the photocatalytic reactions where O_2 is the only or best acceptor (e.g., oxidation of organic compounds) P25 is generally the best material but, when a better acceptor, such as Cr(VI), is present together with an electron donor also well adsorbed on TiO_2, large area samples such as UV100 or PC500 are better materials. A strong effect on the TRMC parameters is observed in P25, attributed again to the anatase-rutile heterojunction, as in other cases [37].

In samples irradiated after contact with Cr(VI) (and EDTA) and submitted to TRMC, I_{max} were similar or somewhat lower than those of HNO_3-modified samples, but higher than those of Cr(VI)-modified and not previously irradiated. This indicates that Cr(III) produced on the surface (last column in Table 2) is less important to change the amount of charge carriers than Cr(VI). There are no large differences in the amount of Cr on the surface among the samples (Table 2), and it is not expected that Cr(III) be an e_{CB}^- acceptor, as the reduction potential of Cr(III) to Cr(II) ($E^0 = -0.42$ V [54]) is more negative than the e_{CB}^- level. In contrast, Cr(III) has been reported to act as a recombination center, thus decreasing the lifetime of charge carriers [32,62,63]. Although Cr(III) has a low absorption in the emission range of the laser [14,64], it can be slightly higher in the presence of EDTA and on the TiO_2 surface; thus, a minor contribution as UV light filter cannot be ruled out, leading to the same effect. An I_{40ns}/I_{max} decrease and a k_D increase is observed in the samples, with the exception of UV100, where some positive effect takes place (a small I_{40ns}/I_{max} increase and a k_D decrease); as the lifetime of charge carriers is much shorter in UV100 than in P25 or PC50, the possible capture of h_{VB}^+ by EDTA (or its by-products) would decrease the high recombination rate of UV100. A smaller deactivation on UV100 than in P25 by Cr(III) deposition has been actually reported [4].

4. Conclusions

The photocatalytic activity of TiO_2 samples for Cr(VI) reduction in the presence of EDTA was evaluated. The temporal Cr(VI) decays support the conclusion that the photocatalytic reduction strongly depends on the nature of the TiO_2 samples, especially on the SSA (except for S230). The final products of the photocatalytic Cr(VI) reduction in the presence of EDTA are Cr(III)–EDTA and Cr on TiO_2, the speciation being almost independent of the photocatalyst; the temporal evolution of Cr(VI) and Cr(III)–EDTA are clearly related.

The results are validated by TRMC, being the first time that this technique was applied to the interpretation of the TiO_2 photocatalytic reduction of metal ions such as Cr(VI). Also, the analysis of the TRMC results with a power decay law has been applied for the first time, giving a more objective analysis of the signals compared with the simple inspection of the graphics. The results show a large decrease in I_{max} and I_D when Cr(VI) is adsorbed in the samples, this effect being more important with the increase of adsorbed Cr(VI). A larger efficiency for e_{CB}^- capture and a UV light filter effect, due to the formation of the Cr(VI)–TiO_2 complex can be responsible for these effects.

Acknowledgments

The authors acknowledge Dr. M. Kunst (Helmholtz Zentrum Berlin, Germany) for his help in TRMC measurements, and Dr. Lidia Pérez and Lic. Alejandra Fontanille for the BET area measurements. This work was performed as part of A11E05 ECOS/MINCyT collaborative project, and Agencia Nacional de Promoción Científica y Tecnológica PICT-512 and PICT-0463 projects.

Appendix A. Supplementary data

Supplementary data associated with this article can be found, in the online version, at http://dx.doi.org/10.1016/j.apcatb.2013.06.032.

References

[1] M.I. Litter, Applied Catalysis B: Environmental 23 (1999) 89–114.
[2] M.I. Litter, Advances in Chemical Engineering 36 (2009) 37–67.
[3] Y. Ku, I.-L. Jung, Water Research 35 (2001) 135–142.
[4] G. Colón, M.C. Hidalgo, J.A. Navío, Journal of Photochemistry and Photobiology A: Chemistry 138 (2001) 79–85.
[5] D. Hufschmidt, D.W. Bahnemann, J.J. Testa, C.A. Emilio, M.I. Litter, Journal of Photochemistry and Photobiology A: Chemistry 148 (2002) 223–231.
[6] U. Siemon, D.W. Bahnemann, J.J. Testa, D. Rodríguez, N. Bruno, M.I. Litter, Journal of Photochemistry and Photobiology A: Chemistry 148 (2002) 247–255.
[7] J.J. Testa, M.A. Grela, M.I. Litter, Environmental Science & Technology 38 (2004) 1589–1594.
[8] J.M. Meichtry, M. Brusa, G. Mailhot, M.A. Grela, M.I. Litter, Applied Catalysis B: Environmental 71 (2007) 101–107.
[9] Y. Di Iorio, E. San Román, M.I. Litter, M.A. Grela, The Journal of Physical Chemistry C 112 (2008) 16532–16538.
[10] J.M. Meichtry, V. Rivera, Y. Di Iorio, E. San Román, M.A. Grela, M.I. Litter, Photochemical & Photobiological Sciences 8 (2009) 604–612.
[11] R. Mu, Z. Xu, L. Li, Y. Shao, H. Wan, S. Zheng, Journal of Hazardous Materials 176 (2010) 495–502.
[12] H.-T. Hsu, S.-S. Chen, Y.-S. Chen, Separation and Purification Technology 80 (2011) 663–669.
[13] M.A. Barakat, Arabian Journal of Chemistry 4 (2011) 361–377.
[14] M. Kebir, M. Chabani, N. Nasrallah, A. Bensmaili, M. Trari, Desalination 270 (2011) 166–173.
[15] Q. Wang, X. Chen, K. Yu, Y. Zhang, Y. Cong, Journal of Hazardous Materials 246–247 (2013) 135–144.
[16] H.-T. Hsu, S.-S. Chen, Y.-F. Tang, H.-C. Hsi, Journal of Hazardous Materials 248–249 (2013) 97–106.
[17] M.C. Hidalgo, G. Colón, J.A. Navío, Journal of Photochemistry and Photobiology A: Chemistry 148 (2002) 341–348.
[18] J. Yoon, E. Shim, S. Bae, H. Joo, Journal of Hazardous Materials 161 (2009) 1069–1074.
[19] N.S. Waldmann, Y. Paz, The Journal of Physical Chemistry C 114 (2010) 18946–18952.
[20] A. Idris, N. Hassan, N.S.M. Ismail, E. Misran, N.M. Yusof, A.-F. Ngomsik, A. Bee, Water Research 44 (2010) 1683–1688.
[21] A. Pandikumar, R. Ramaraj, Journal of Hazardous Materials 203–204 (2011) 244–250.
[22] A. Kleiman, M.L. Vera, J.M. Meichtry, M.I. Litter, A. Márquez, Applied Catalysis B: Environmental 101 (2011) 676–681.
[23] R. Gherbi, N. Nasrallah, A. Amrane, R. Maachi, M. Trari, Journal of Hazardous Materials 186 (2011) 1124–1130.
[24] M.V. Dozzi, A. Saccomanni, E. Selli, Journal of Hazardous Materials 211–212 (2012) 188–195.
[25] S. Liu, N. Zhang, Z.R. Tang, Y.J. Xu, ACS Applied Materials & Interfaces 4 (2012) 6378–6385.
[26] G. Chen, M. Sun, Q. Wei, Z. Ma, B. Du, Applied Catalysis B: Environmental 125 (2012) 282–287.
[27] Y.C. Zhang, J. Li, H.Y. Xu, Applied Catalysis B: Environmental 123–124 (2012) 18–26.
[28] P.S. Suchithra, C.P. Shadiya, A. Peer Mohamed, P. Velusamy, S. Ananthakumar, Applied Catalysis B: Environmental 130–131 (2013) 44–53.
[29] A.E. Giannakas, E. Seristatidou, Y. Deligiannakis, I. Konstantinou, Applied Catalysis B: Environmental 132–133 (2013) 460–468.
[30] J. Kuncewicz, P. Ząbek, K. Kruczała, K. Szaciłowski, W. Macyk, The Journal of Physical Chemistry C 116 (2012) 21762–21770.
[31] K.-M. Schindler, M. Kunst, The Journal of Physical Chemistry 94 (1990) 8222–8226.
[32] C. Colbeau-Justin, M. Kunst, D. Huguenin, Journal of Materials Science 38 (2003) 2429–2437.
[33] Yu.V. Kolen'ko, A.V. Garshev, B.R. Churagulov, S. Boujday, P. Portes, C. Colbeau-Justin, Journal of Photochemistry and Photobiology A: Chemistry 172 (2005) 19–26.
[34] S. Boujday, F. Wünsch, P. Portes, J.-F. Bocquet, C. Colbeau-Justin, Solar Energy Materials & Solar Cells 83 (2004) 421–433.
[35] G. Mele, R. Del Sole, G. Vasapollo, G. Marci, E. García-López, L. Palmisano, J.M. Coronado, M.D. Hernández-Alonso, C. Malitesta, M.R. Guascito, The Journal of Physical Chemistry B 109 (2005) 12347–12352.
[36] M. Kunst, F. Goubard, C. Colbeau-Justin, F. Wünsch, Materials Science and Engineering C 27 (2007) 1061–1064.
[37] C.A. Emilio, M.I. Litter, M. Kunst, M. Bouchard, C. Colbeau-Justin, Langmuir 22 (2006) 3606–3613.
[38] E. Kowalska, H. Remita, C. Colbeau-Justin, J. Hupka, J. Belloni, The Journal of Physical Chemistry C 112 (2008) 1124–1131.
[39] C. Wei, S. German, S.R. Basak, K. Rajeshwar, Journal of the Electrochemical Society 140 (1993) 2477–2482.
[40] Z. Marczenko, M. Balcerzak, Separation, Preconcentration, and Spectrophotometry in Inorganic Analysis, Analytical Spectroscopy Library, Elsevier, Amsterdam, 2000, pp. 159–166.
[41] A.D. Bokare, W. Choi, Environmental Science & Technology 45 (2011) 9332–9338.
[42] K.A. Easom, R.N. Bose, Inorganic Chemistry 27 (1988) 2331–2334.
[43] Y. Fuji, E. Kyuno, R. Tsuchiya, Bulletin of the Chemical Society of Japan 42 (1969) 1569–1572.
[44] Y. Fuji, E. Kyuno, R. Tsuchiya, Bulletin of the Chemical Society of Japan 43 (1970) 786–789.
[45] A. Uehara, E. Kyuno, R. Tsuchiya, Bulletin of the Chemical Society of Japan 43 (1970) 1394–1397.
[46] P.A. Babay, C.A. Emilio, R.E. Ferreyra, E.A. Gautier, R.T. Gettar, M.I. Litter, Water Science and Technology 44 (2001) 179–185.
[47] P.A. Babay, C.A. Emilio, R.E. Ferreyra, E.A. Gautier, R.T. Gettar, M.I. Litter, International Journal of Photoenergy 3 (2001) 193–199.
[48] M.I. Cabrera, O.M. Alfano, A.E. Cassano, Journal of Physical Chemistry 100 (1996) 20043–20050.
[49] C. Guillard, E. Puzenat, H. Lachheb, A. Houas, J.-M. Herrmann, International Journal of Photoenergy 7 (2005) 1–9.
[50] D. Gumy, C. Morais, P. Bowen, C. Pulgarin, S. Giraldo, R. Hajdu, J. Kiwi, Applied Catalysis B: Environmental 63 (2006) 76–84.
[51] J. Ryu, W. Choi, Environmental Science & Technology 42 (2008) 294–300.
[52] C.B. Mendive, T. Bredow, A. Feldhoff, M.A. Blesa, D.W. Bahnemann, Physical Chemistry Chemical Physics 11 (2009) 1794–1808.
[53] S.-M. Lee, I.-H. Cho, Y.-Y. Chang, J.-K. Yang, Journal of Environmental Science and Health Part A 42 (2007) 543–548.
[54] I. Dellien, F.M. Hall, L.G. Hepler, Chemical Reviews 76 (1976) 283–310.
[55] S.T. Martin, H. Herrmann, M.R. Hoffmann, Journal of the Chemical Society, Faraday Transactions 90 (1994) 3323–3330.
[56] N. Wang, Y. Xu, L. Zhu, X. Shen, H. Tang, Journal of Photochemistry and Photobiology A: Chemistry 201 (2009) 121–127.
[57] S. Tuprakay, W. Liengcharernsit, Journal of Hazardous Materials B 124 (2005) 53–58.
[58] P. Wardman, Journal of Physical and Chemical Reference Data 18 (1989) 1637–1755.
[59] R.W. Fessenden, D. Meisel, D.M. Camaioni, Journal of the American Chemical Society 122 (2000) 3773–3774.
[60] H.H. Mohamed, C.B. Mendive, R. Dillert, D.W. Bahnemann, The Journal of Physical Chemistry 115 (2011) 2139–2147.
[61] V.N.H. Nguyen, R. Amal, D. Beydoun, Chemical Engineering Science 60 (2005) 5759–5769.
[62] J.M. Herrmann, J. Disdier, P. Pichat, Chemical Physics Letters 108 (1984) 618–622.
[63] J. Disdier, J.M. Hermann, P. Pichat, Langmuir 10 (1994) 643–652.
[64] B. Li, A. Lin, X. Wu, Y. Zhang, F. Gan, Journal of Alloys and Compounds 453 (2008) 93–101.